Remote Sensing of Fractional Snow Cover Using Moderate Resolution Imaging Spectroradiometer (MODIS) Data

JONATHAN S. BARTON,[1] DOROTHY K. HALL,[2] AND GEORGE A. RIGGS[3]

ABSTRACT

The Earth Observing System Terra spacecraft, launched on December 18, 1999, includes the Moderate Resolution Imaging Spectroradiometer (MODIS) in its instrument payload. By summer 2000, 500-m-resolution snow-cover maps will be produced daily and archived and distributed at the National Snow and Ice Data Center in Boulder, Colorado. These maps should represent an improvement over existing snow-cover maps. One significant improvement is the development of an algorithm to produce fractional snow cover within each pixel. A binary snow map is produced using the normalized difference snow index (NDSI) and the normalized difference vegetation index (NDVI) using a grouped-criteria-technique algorithm that employs four MODIS bands. In one of several methods under development, fractional snow cover using NDSI and NDVI was compared with fractional snow cover calculations from spectral unmixing of a Landsat Thematic Mapper image of the Sierra Nevada near Mono Lake, California. Preliminary results from the spectral unmixing comparison show that the algorithm is capable of mapping fractional snow cover to within ±10% of the unmixing results. The fractional snow-cover-mapping algorithm has also been tested in other areas using Landsat thematic mapper data, and for North America using MODIS data. A correction to the NDSI for cirrus cloud cover was developed and applied to aircraft data from the MODIS Airborne Simulator.

Key Words: MODIS, Snow, Snow-covered area

INTRODUCTION

The Moderate-Resolution Imaging Spectroradiometer (MODIS), launched on the Terra platform in December 1999, will produce daily snow maps of the globe at 500-m resolution. To make these maps, the algorithm utilizes the Normalized Difference Snow Index (NDSI, Eq 1), and the Normalized Difference Vegetation Index (NDVI, Eq 2) for classification (Hall et al. 1998). To increase the value of this product to potential users, several independent efforts are being made to include an estimation of the percentage of each pixel covered by snow or fractional snow cover.

[1] General Sciences Corporation, 4600 Powder Mill Road, Suite 400, Beltsville, Maryland 20705, USA
email: Jonathan.S.Barton@gsfc.nasa.gov

[2] NASA/Goddard Space Flight Center, Code 974, Hydrological Sciences Branch, Greenbelt, Maryland 20771, USA

[3] Research & Data Systems Corporation, 7833 Walker Drive, Suite 550, Greenbelt, Maryland 20770, USA

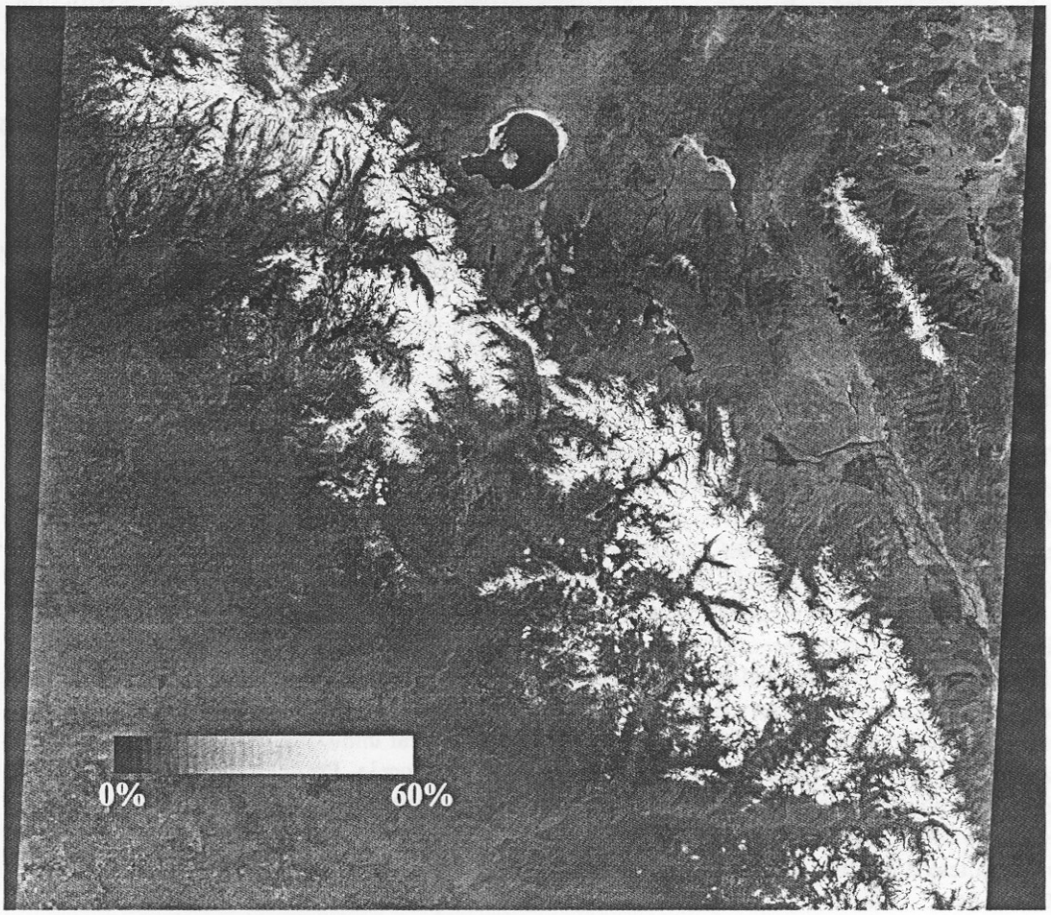

Figure 1.
The 0.55 mm (Band 2) reflectance of the 10 May 1992 Landsat Thematic Mapper (TM) scene of the Sierra Nevada near Mono Lake. Band 2 saturates at about 60% reflectance.

$$NDSI = \frac{\rho_{0.55\mu m} - \rho_{1.6\mu m}}{\rho_{0.55\mu m} + \rho_{1.6\mu m}} \quad (1)$$

$$NDVI = \frac{\rho_{0.83\mu m} - \rho_{0.66\mu m}}{\rho_{0.83\mu m} + \rho_{0.66\mu m}} \quad (2)$$

Where ρ_i indicates the unitless exoatmospheric reflectance at the wavelength *i*.

Fractional snow cover is an important element in mesoscale climate modeling calculations, as well as in snowmelt runoff modeling.

MAPPING FRACTIONAL SNOW COVER

The data selected for the derivation of the algorithm was the 10 May 1992 Landsat-5 Thematic Mapper scene, path 42, row 34. No atmospheric corrections were made on the scene. This scene was selected because of the availability of existing spectral unmixing endmembers calculated by Rosenthal (1993). These endmembers are provided in Table 1.

Table 1. Reflectance Endmembers for Spectral Unmixing from Rosenthal (1993).

Category	TM Band 1	TM Band 2	TM Band 3	TM Band 4	TM Band 5	TM Band 7
Rock	0.175	0.210	0.250	0.310	0.395	0.400
Vegetation	0.009	0.024	0.020	0.505	0.130	0.055
Snow	0.205	0.540	0.450	0.680	0.008	0.009

In order to obtain a ground-truth dataset, spectral unmixing was performed using Research Systems Inc.'s Environment for Visualizing Images (ENVI) and the endmembers in Table 1. The unmixing was run using an unconstrained single-value decomposition on a linear unmixing model. This spectral unmixing resulted in a ground-truth estimate of the percentage of snow (SCA) (Figure 1.), vegetation and rock for each pixel in the scene. In order to create an algorithm for the calculation of the fractional snow cover from the NDSI, the snow cover percent from the spectral unmixing was then plotted against the NDSI, and 2000 samples from each 10% range of snow cover percents, randomly selected, (20000 samples total) were used for the polynomial regression calculation. (Figure 2.)

$$FSC = 0.180 + 0.371NDSI + 0.255NDSI^2 \quad (3)$$

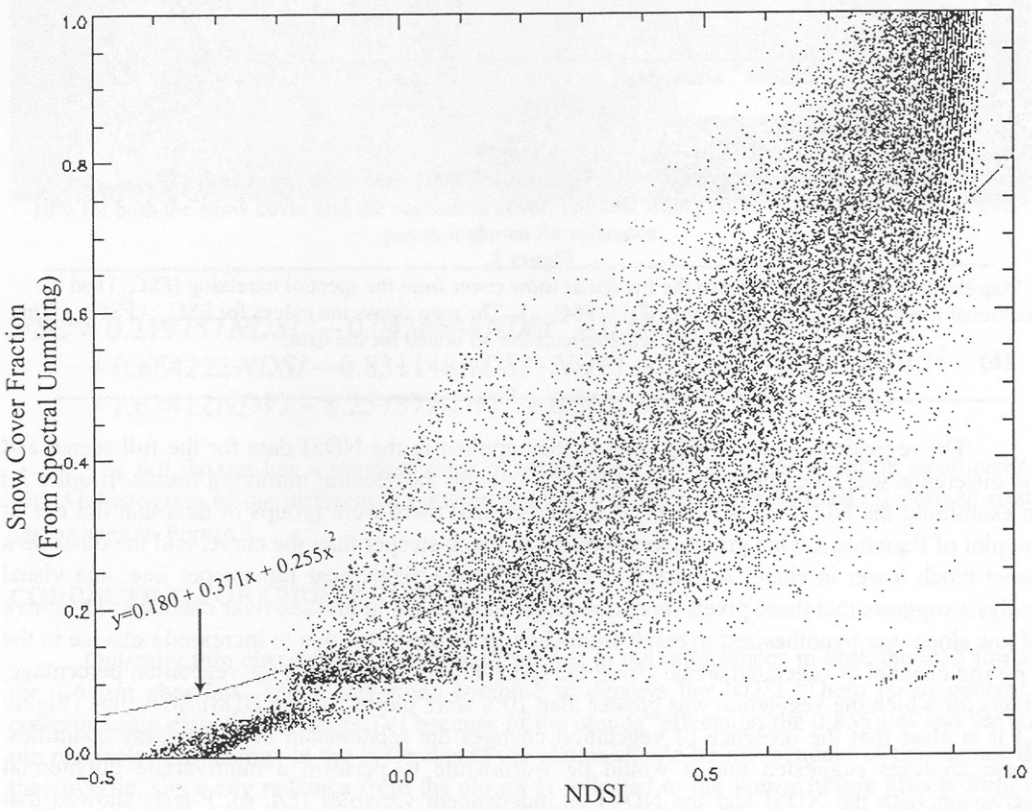

Figure 2.
Plot of the 20000 selected data points from the 10 May 1992 TM scene used to develop the algorithm. The points were selected as 2000 random samples from each 10% snow cover catagory (from the spectral unmixing), in order to ensure that the whole range of values was represented. The plot of Equation 2 is shown for reference.

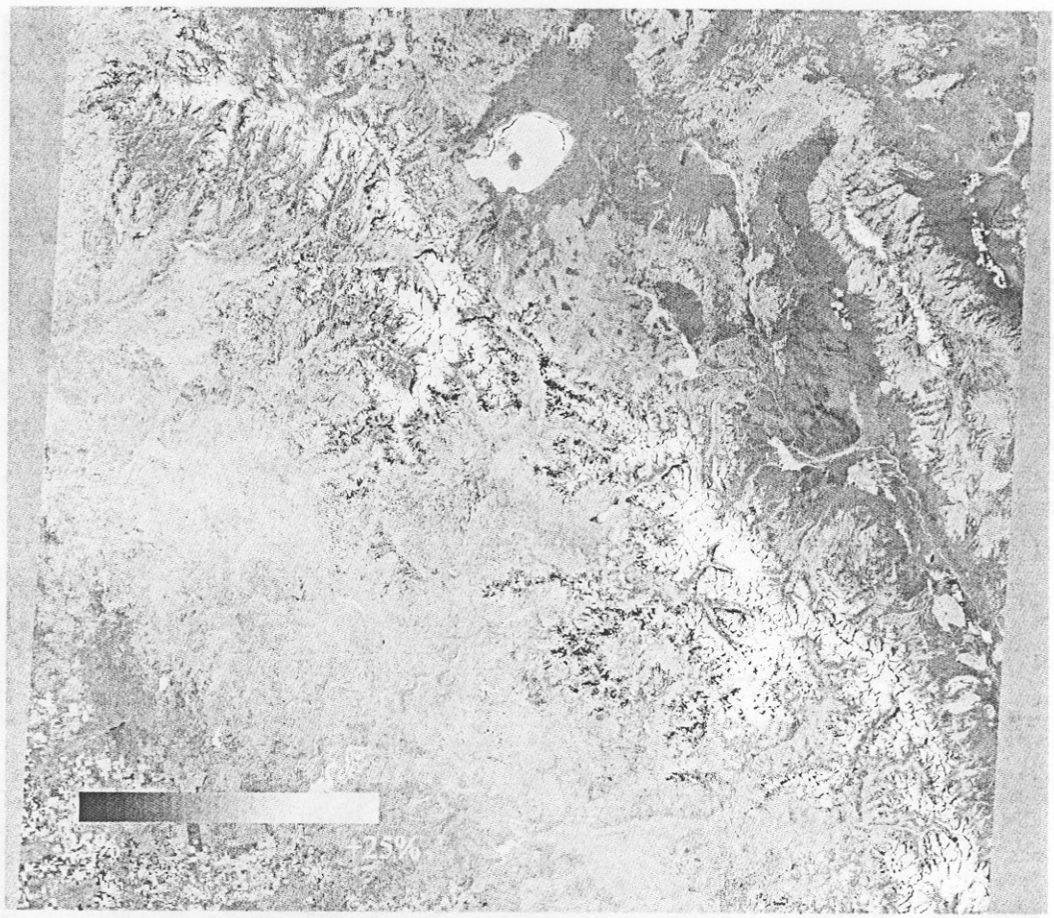

Figure 3.
Map showing differences between the fractional snow cover from the spectral unmixing (FSC_{SU}) and the fractional snow cover derived from the NDSI (FSC_{NDSI}). The map shows the values for FSC_{SU} - FSC_{NDSI}. The ±25% color scale reflects the 3σ bound for the data.

The regression equation (Eq. 3) was then applied to the NDSI data for the full scene, and the difference was taken between the NDSI product and the spectral unmixing results. (Figure 3.) In examining the NDSI vs. SCA plot, it was noted that there were groups of data that did not fit the plot of Equation 2. One group plotted on a line much steeper than the curve, and the other on a curve much lower in slope. A mask was created for the pixels near the steeper line, and visual analysis suggests that these pixels represent sands and gravels in braided river channels. The curve of low slope was hypothesized to result from changes in the NDSI due to increased radiance in the 1.65 μm channel in vegetated areas. Using the spectral unmixing results for vegetation percentage, pixels for which the vegetation was greater than 10% were plotted on the NDSI/SCA plot. (Figure 4.) It is clear that the presence of vegetation changes the relationship between these quantities. These analyses suggested that it would be worthwhile to perform a multivariate polynomial regression with the NDSI and the NDVI as independent variables (Eq. 4). F-tests showed that using the NDVI significantly improved the fit of the estimated fractional snow cover to the spectral unmixing results. A difference map from these new results is shown in Figure 5. The inset shows that the error is related systematically to elevation, which in this scene is also highly correlated with the fractional snow cover.

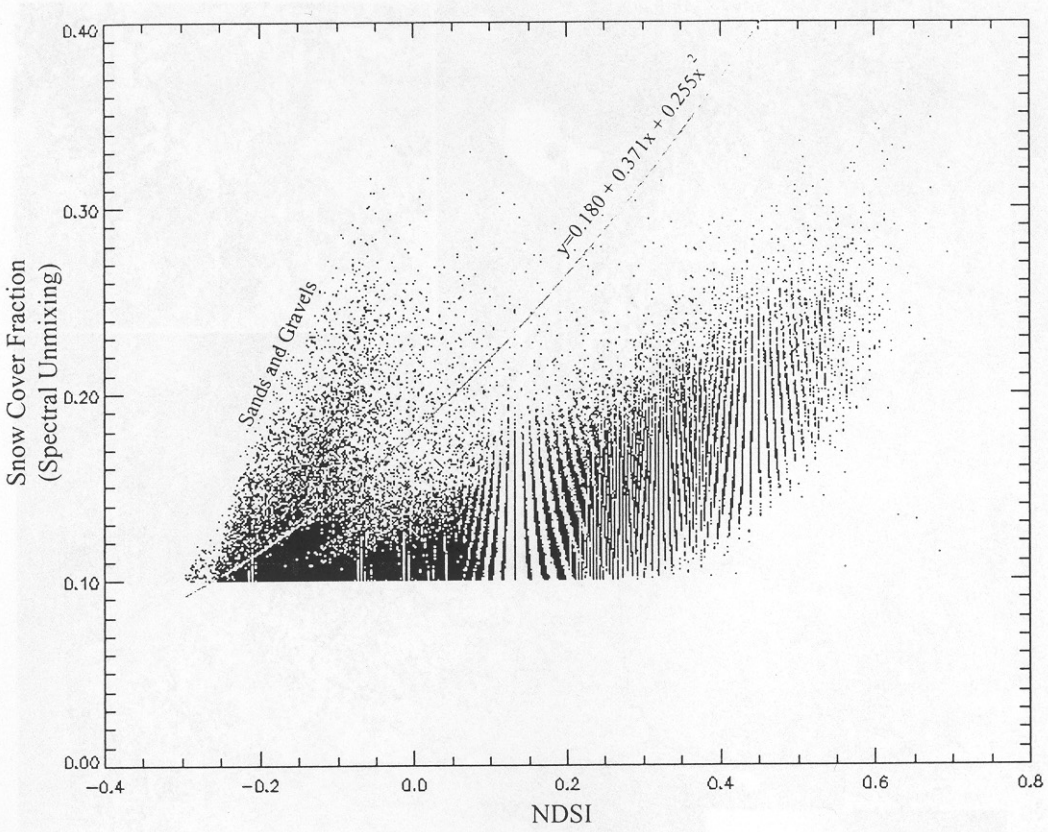

Figure 4.
Plot showing all points from the 10 May 1992 TM scene for which spectral unmixing returns greater than 10% for both the snow cover and the vegetation cover. The best fitting curve to the 20000 selected data points is shown for reference.

$$FSC = 0.219757NDSI^3 - 0.0436684NDSI^2 - 0.600878NDSI^2NDVI \cdot \\ + 0.684222NDSI - 0.831148NDSI \cdot NDVI - 2.55949NDSI \cdot NDVI^2 \\ + 1.67412NDVI - 8.25737NDVI^2 + 8.30125NDVI^3 + 0.124414 \quad (4)$$

The full dataset has a standard error of estimate of 5.56%, and an absolute mean error of 3%. An histogram of the differences between the spectral unmixing and the NDSI-derived results can be seen in Figure 6.

CORRECTING FOR CIRRUS CLOUD COVER

Optically thin cirrus clouds produce elevations in the reflectances in both the 0.55 μm and the 1.6 μm channels. These elevations combine to depress the NDSI. There is, in general, a corresponding elevation in the NDVI because of the clouds' effects on the 0.855 μm and the 0.65 μm channels. The change in the index due to the clouds should be independent of the surface that they overlie, since any radiance from the clouds is reflected to the sensor before effects from the surface are applied. Thus a single correction can be applied to all values of the FSC for given cirrus cloud opacity, as represented by the reflectance in a water vapor absorption band.

There has been substantial literature (e.g. Gao and Geotz, 1993, Ackerman et al., 1997) on the detection of cirrus clouds using water vapor absorption bands, and so the details will only be summarized here. Because nearly all of the energy in these bands is absorbed in the lower atmosphere, all of the radiance received by the satellite must come from high-level cirrus clouds.

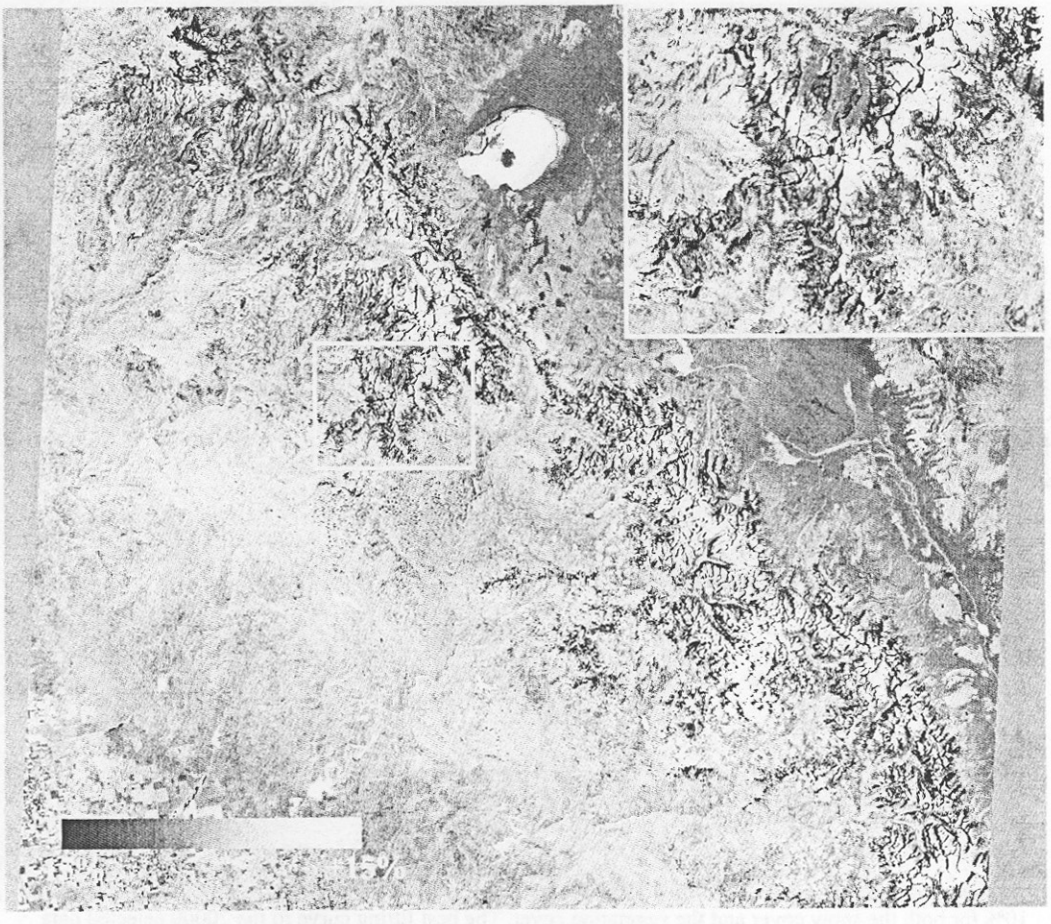

Figure 5.
Difference map showing how the NDSI/NDVI derived results (FSC_{NDSI}) compare with the spectral unmixing results (FSC_{SU}). This map shows the result of the difference FSC_{SU} - FSC_{NDSI}. The detail (inset) shows the systematic increase in error along the ridges, where the fractional snow cover is greater. Note that the -15% to +15% scale selected for this map reflects the $\pm 3\sigma$ bound of the data.

Preliminary work was done using MODIS Airborne Simulator (MAS) data, since MODIS data was not yet available. The MAS is flown on the NASA ER-2 high-altitude aircraft, and provides data similar to that which will be available from MODIS. (Gumley, et al. 1994.) The water vapor absorption channel available on MAS is a 1.889 μm band. MODIS has a 1.375 μm channel that is expected to work similarly to the 1.889 μm band on MAS for cirrus cloud detection (Ackerman et al., 1997).

Figure 7 shows the reflectance in the 1.889 μm water vapor absorption channel (band 15) for the Winter Cloud Experiment (WINCE) Flight #97-042, Track 8 acquired 29 January 1997: The areas of high reflectance correspond to the areas of cirrus cloud. Figures 8a and 8b show the uncorrected NDSI and NDVI (respectively) for the scene, while Figure 8c shows the results of the FSC algorithm using these scenes.

Several assumptions were necessary to create a relationship between the cirrus cloud cover, as measured by the reflectance in the 1.889 μm channel ($\rho_{1.889}$) and the NDSI. First, it was assumed, with few reservations, that the cirrus cloud cover and the snow cover percentage were not correlated. Second, it was assumed, for simplicity, that at a given $\rho_{1.889}$, the only controlling factor of the NDSI was the snow cover percent. Third, it was assumed that cirrus cloud cover

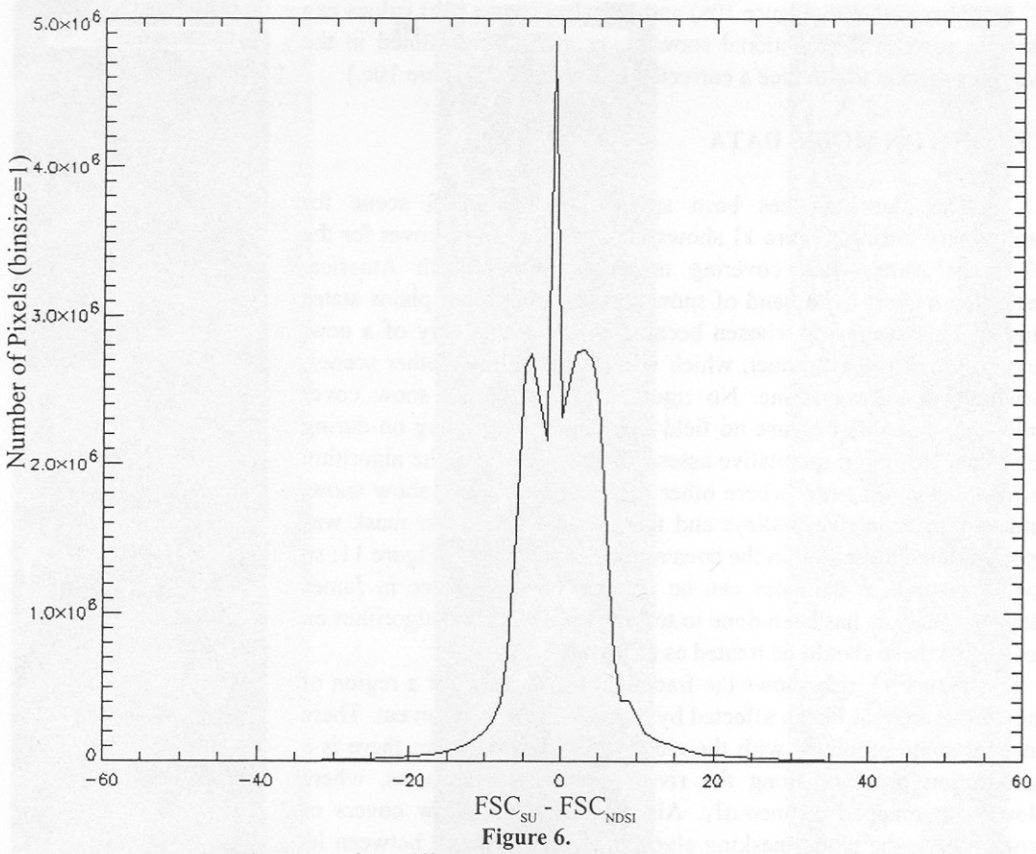

Figure 6.
Histogram of the difference map shown in Figure 5. σ is 5.56.

would depress the NDSI equally for all snow cover percent. Using these assumptions, it was possible to plot a line (Equation 5.) showing the decrease in the NDSI with increasing $\rho_{1.889}$

$$NDSI_c = NDSI + 2.67284\rho_{1.889} \quad \textbf{(5)}$$

where $NDSI_c$ represents a corrected NDSI.

Figure 9 shows this plot, along with the corresponding plot showing the elevation of the NDVI using a corresponding assumption for the minimum NDVI. It was observed that for small values of $\rho_{1.889}$, there was an observed depression of the NDVI, but for larger values, the index was depressed. This is probably due to a depression in the radiance in one of the bands used to calculate the NDVI and an elevation in the other, and each dominates the effect at different levels of $\rho_{1.889}$. Since the relationship for the NDVI was not as simple as that for the NDSI, three lines were determined to fit the data for different ranges of $\rho_{1.889}$. (Equation 5).

$$NDVI_c = \begin{cases} \rho_{1.889} < 0 & NDVI \\ 0 \le \rho_{1.889} < 0.3 & NDVI - 0.409077\rho_{1.889} \\ 0.3 \le \rho_{1.889} < 0.7 & NDVI + 0.714714\rho_{1.889} - 0.0362792 \\ 0.7 \le \rho_{1.889} \le 1.0 & NDVI + 0.270219\rho_{1.889} - 0.00688379 \\ \rho_{1.889} > 1.0 & NDVI \end{cases} \quad \textbf{(6)}$$

These NDSIc (Figure 10a) and NDVIc (Figure 10b) values can then be used in the fractional snow cover algorithm outlined in the previous section to produce a corrected FSC product. (Figure 10c.)

TESTING ON MODIS DATA

The algorithm has been applied to a MODIS scene for preliminary testing. Figure 11 shows the fractional snow cover for the 08 April 2000 swath covering northern central North America, including a short-lived band of snow across the northern plains states (inset). This scene was chosen because of the availability of a new, revised cloud mask product, which was unavailable for other scenes, when the work was done. No rigorous testing of the snow cover amount is possible because no field campaigns were going on during this time. However, qualitative assessment suggests that the algorithm is mapping more snow where other mapping techniques show snow, and less snow in river valleys and the like. No land/water mask was applied to the algorithm in the construction of the map in Figure 11; so ice concentration estimates can be mapped on the sea ice in James Bay. No analysis has been done to test the validity of the algorithm on sea ice, so these should be treated as estimates.

Figure 11 also shows the fractional snow cover for a region of the northern Great Plains affected by a single snow storm event. There are still some problems with the cloud mask; in particular, there is a geolocation problem along the rivers and lake boundaries, where clouds are mapped erroneously. Also, in fractional snow covers of around 40%, the cloud-masking algorithm is in transition between its cloud-over-snow processor and its cloud-over-land processor, and maps some fractionally snow-covered pixels as cloudy.

CONCLUSIONS AND FUTURE WORK

When the results of the algorithm were compared with the original spectral unmixing data, a 95% confidence of ±11% was obtained. The error is much less at low percentages of snow cover, and higher in areas of greater percent snow cover.

Over all, the fractional snow cover algorithm seems to be mapping snow in the right areas. Some adjustment is needed in the algorithm because of the tendency to underestimate coverage in areas of high snow cover. However, as this is a systematic error, it may be possible to make a correction for this effect.

The corrections for cirrus clouds discussed in this paper should make it possible to map fractional snow, and binary snow, more accurately through thin cirrus clouds. Because cirrus clouds cover a substantial portion of the globe each day, this will be a useful addition to the algorithm.

The bulk of the future work planned for this algorithm will be

Figure 7.
1.889 μm reflectance for the 29 January 1997 MODIS Airborne Simulator WINCE Flight 97-042, Track 08. Brighter areas indicate the presence of cirrus clouds.

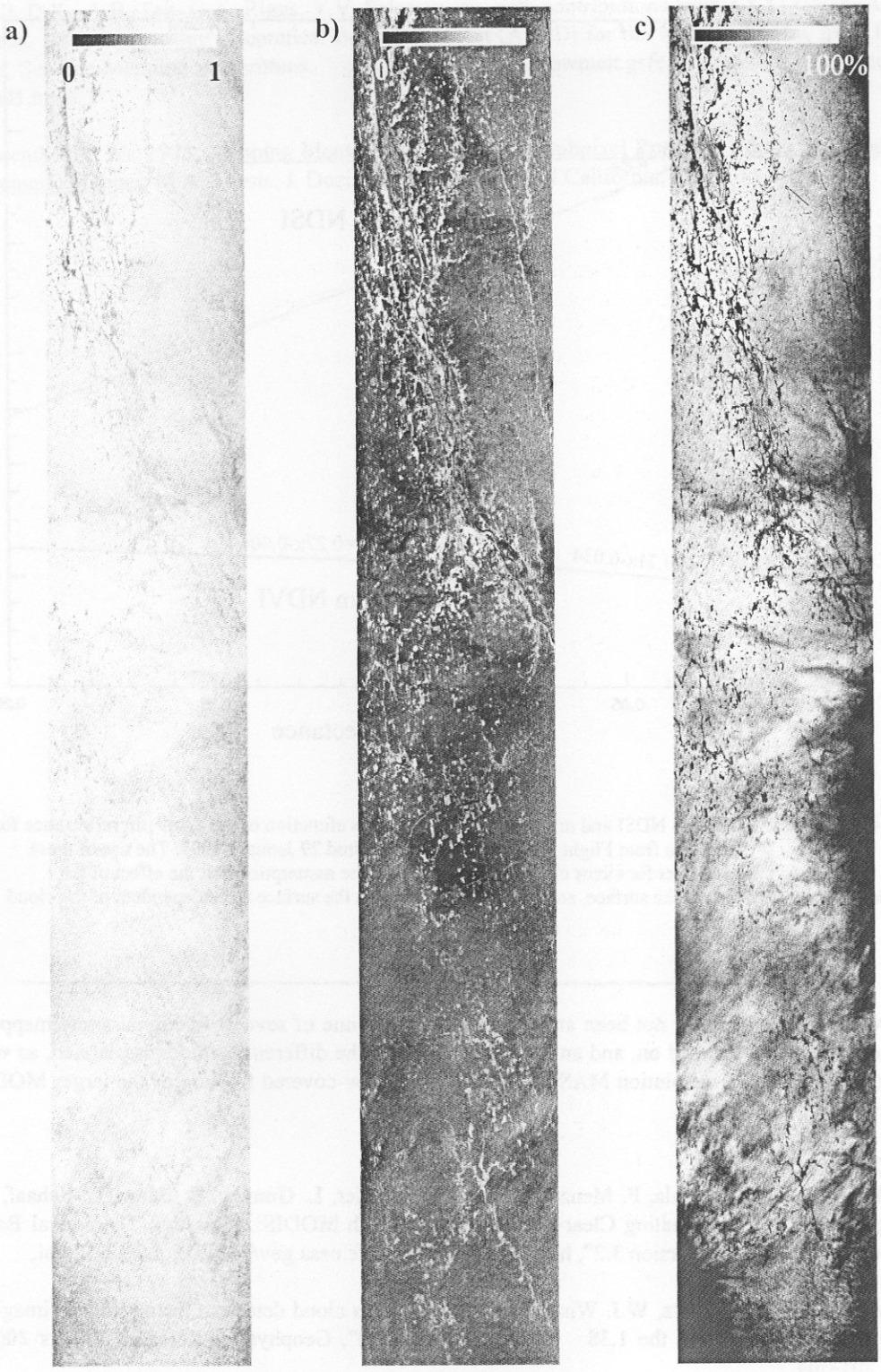

Figure 8.
Uncorreced algorithm results for the MODIS Airborne Simulator WINCE Flight 97-042, Track 08.
a) Uncorrected NDSI. b) Uncorrected NDVI. c) Fractional Snow Cover calculated using the uncorrected indices and Equation3.

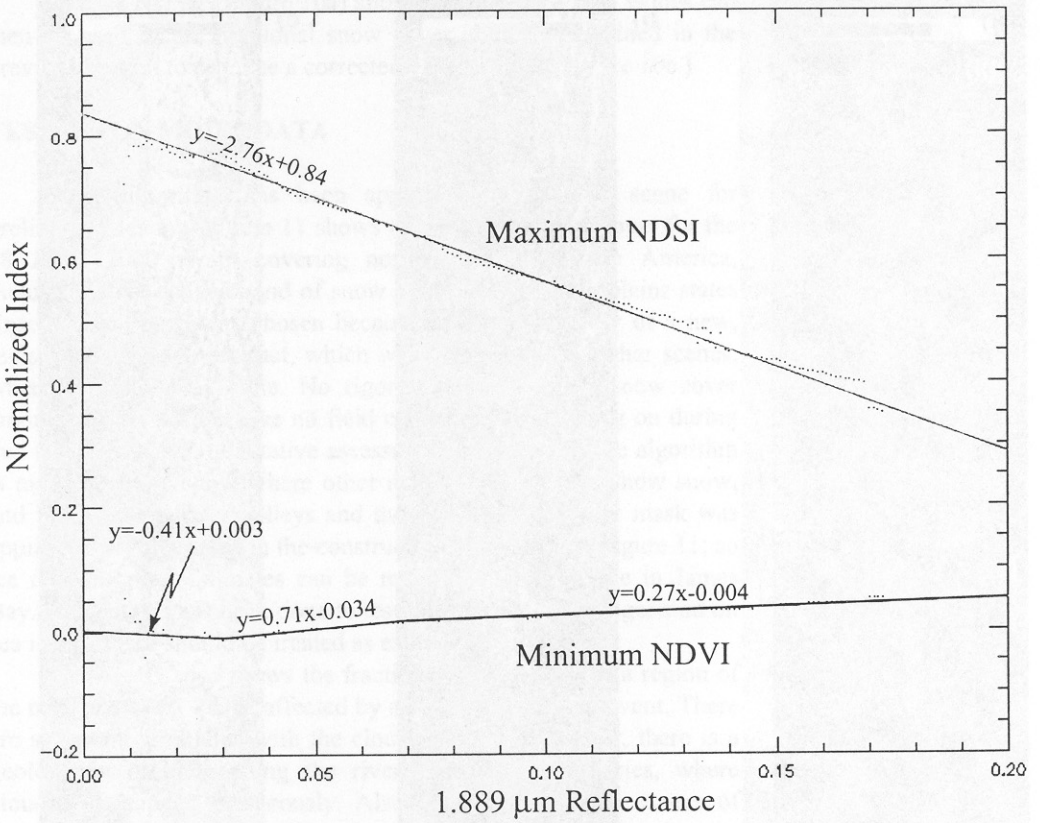

Figure 9.
Plot showing the maximum NDSI and minimum NDVI values as afunction of the 1.889 µm reflectance for the MAS - WINCE data from Flight 97-042, Track 08, acquired 29 January 1997. The use of these regressions to correct for cirrus clouds is contingent on the assumption that the effect of the clouds is independent of the surface, and that the conditions on the surface are independent of the cloud cover.

in validation, which has not been attempted yet. This is one of several fractional snow mapping algorithms being worked on, and an intercomparison of the different methods is planned, as well as the use of higher resolution MAS data to map the snow-covered fraction of the larger MODIS pixels.

REFERENCES

Ackerman, S., K. Strabala, P. Menzel, R. Frey, C. Moeller, L. Gumley, B. Baum, C. Schaaf, G. Riggs, 1997: "Discriminating Clear-Sky from Cloud with MODIS: Algorithm Theoretical Basis Document (MOD35) Version 3.2", http://modis-atmos.gsfc.nasa.gov/MOD35_L2/atbd.html.

Gao, B.-C., A.F.H. Goetz, W.J. Wiscombe, 1993: "Cirrus cloud detection from airborne imaging spectrometer data using the 1.38 m water vapor band", Geophysical Research Letters **20**(4), pp. 301-304.

Gumley, L.E. P.A. Hubanks, E.J. Masuokam 1994: "MODIS Technical Report Series, Volume 3: MODIS Airborne Simulator Level 1B Data User's Guide", NASA Technical Memorandum 104594, Volume 3.

Hall, D.K., A.B. Tait, G.A. Riggs, V.V. Salomonson, with contributions from J.Y.L. Chien, A.G. Klein, 1998: "Algorithm Theoretical Basis Document (ATBD) for the MODIS Snow-, Lake Ice- and Sea Ice-Mapping Algorithms. Version 4.0", http://snowmelt.gsfc.nasa.gov/MODIS_Snow/atbd1.html.

Rosenthal, C.W., 1993: Mapping Montane Snow Cover at Subpixel Resolution from the Landsat Thematic Mapper, M.A. Thesis, J. Dozier, adv., University of California, Santa Barbara.

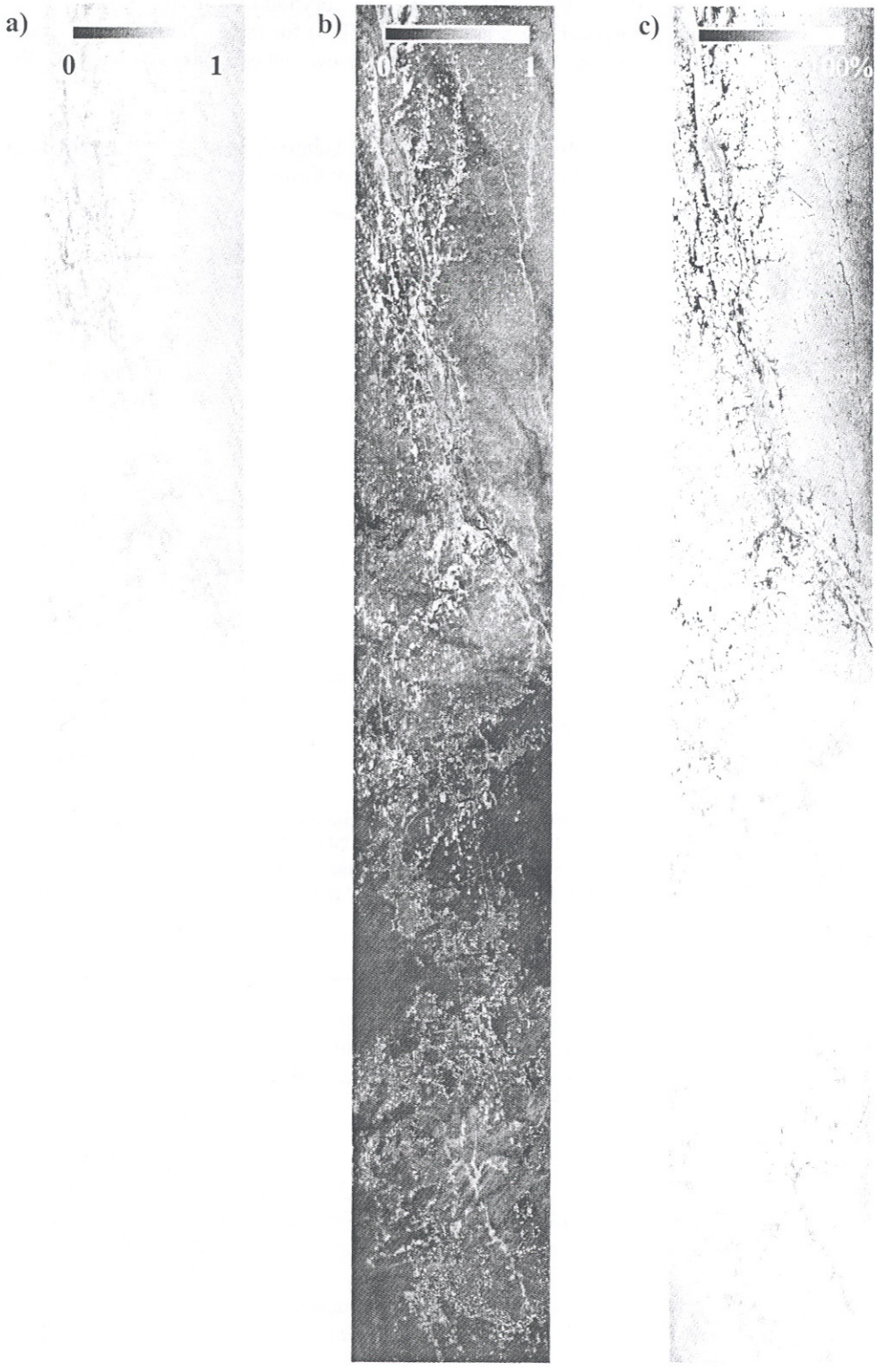

Figure 10.
Correced algorithm results for the MODIS Airborne Simulator WINCE Flight 97-042, Track 08. a) Corrected NDSI. b) Corrected NDVI. c) Fractional Snow Cover calculated using the corrected indices and Equation 3.

Figure 11.
Fractional snow cover for the 08 April 2000 MODIS swath covering northern central North America. Clouds are shown in white.